Biophysical Journal, Volume 96

Supporting Material

The elastic basis for the shape of Borrelia burgdorferi

Christopher Dombrowski, Wanxi Kan, Md. Abdul Motaleb, Nyles W. Charon, Raymond E. Goldstein, and Charles W. Wolgemuth

The elastic basis for the shape of *Borrelia burgdorferi*

Supplemental Material

C. Dombrowski, W. Kan, Md. A. Motaleb, N. W. Charon, R. E. Goldstein, and C. W. Wolgemuth

1 The mathematical model

Differential geometry of the cell cylinder and periplasmic flagella

In this Supplemental Material section, we derive the mathematical model for the unstressed shape of *B. burgdorferi*. We begin by defining the local geometry of the cell cylinder (CC) and the periplasmic flagella (PF). Constraining the flagella to reside at the surface of the cell cylinder provides a relationship between the centerline coordinates of the CC and the PF. We use linear elasticity to define the elastic restoring torques and forces for the CC and the PF. Force and torque balance then leads to a coupled system of ordinary differential equations (ODEs) that determines the morphology of the CC and the PF.

Since the CC and the PF are much longer than they are wide, we treat them both as filamentary objects with circular cross-sections. There are typically between 7 and 11 PFs per end in *B. burgdorferi* (1). For simplicity, we will treat these flagella as a single filament. We define the centerline of the CC as $\mathbf{r}_c(s)$, where s is the arclength along the centerline (Figure 1). Likewise, $\mathbf{r}_f(s_f)$ is the centerline position of the PF, where s_f is the arclength along the flagellar filament (Figure 1).

At all points along the centerline of the CC, we define an orthonormal triad $\{\hat{\mathbf{e}}_1, \hat{\mathbf{e}}_2, \hat{\mathbf{e}}_3\}$, with $\hat{\mathbf{e}}_3 = \partial \mathbf{r}_c/\partial s$ the tangent vector of the CC. The unit vectors $\hat{\mathbf{e}}_1$ and $\hat{\mathbf{e}}_2$ point to material points on the surface of the cell cylinder

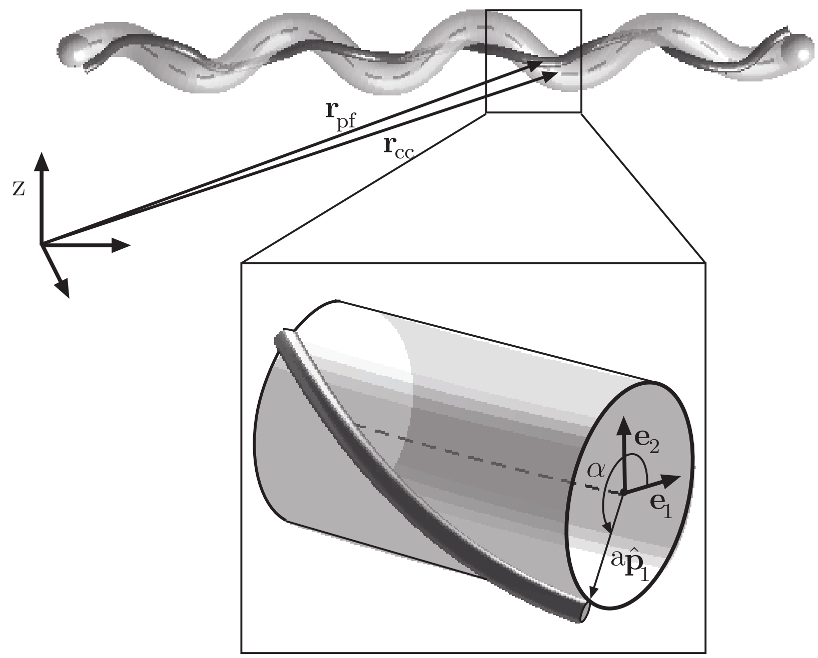

Figure 1: Schematic diagram showing a *B. burgdorferi* cell. The cell cylinder is grey and the periplasmic flagella are treated as a single helical filament, shown in black. The centerline of the cell cylinder, described by the vector $\mathbf{r}_c$, is depicted by the dashed line. $\mathbf{r}_f$ is the vector describing the centerline of the periplasmic flagella. (Inset) A close up view of a short segment of the cell. $\hat{\mathbf{e}}_1$ and $\hat{\mathbf{e}}_2$ are unit vectors that point to the surface of the cell cylinder. The flagella are located at a point $a\hat{\mathbf{p}}_1$ from the centerline. α is the angle from $\hat{\mathbf{e}}_1$ to $\hat{\mathbf{p}}_1$.

(Figure 1). As the CC bends and twists, the positions of these material points change, causing the material frame to rotate (2):

$$\frac{\partial \hat{\mathbf{e}}_i}{\partial s} = \mathbf{\Omega} \times \hat{\mathbf{e}}_i \tag{S1}$$

where $i = 1, 2, 3$. The vector $\mathbf{\Omega} = \{\Omega_1, \Omega_2, \Omega_3\}$ is the strain vector, which describes the bending and twisting strain at a given point. Ω_1 and Ω_2 give the curvature of the CC and Ω_3 is the twist of the CC about the tangent vector.

Since the PF lie at the surface of the CC, we can describe the position of the PF in terms of $\mathbf{r}_c$ (Figure 1),

$$\mathbf{r}_f = \mathbf{r}_c + a\cos\alpha\hat{\mathbf{e}}_1 + a\sin\alpha\hat{\mathbf{e}}_2 = \mathbf{r}_c + a\hat{\mathbf{p}}_1 \ , \tag{S2}$$

where a is the radius of the CC and α is the angular position of the PF with respect to $\hat{\mathbf{e}}_1$. It is useful to define the unit vector $\hat{\mathbf{p}}_1$ that points from the centerline of the CC to the PF. The tangent vector of the PF is $\hat{\boldsymbol{\epsilon}}_3 = \partial\mathbf{r}_f/\partial s_f$, which can be related to the CC variables using Eqs. S1 & S2,

$$\begin{aligned}
\hat{\boldsymbol{\epsilon}}_3 &= \frac{1}{\sqrt{g}}\frac{\partial \mathbf{r}_f}{\partial s} \\
&= \frac{1}{\sqrt{g}}\left(-a\left(\Omega_3 + \frac{\partial\alpha}{\partial s}\right)\sin\alpha\hat{\mathbf{e}}_1 + a\left(\Omega_3 + \frac{\partial\alpha}{\partial s}\right)\cos\alpha\hat{\mathbf{e}}_2\right. \\
&\quad \left. + \left(1 - a\Omega_2\cos\alpha + a\Omega_1\sin\alpha\right)\hat{\mathbf{e}}_3\right) \ ,
\end{aligned} \tag{S3}$$

where $\sqrt{g}$ is the ratio between a differential arclength along the PF to a differential arclength along the CC; i.e.,

$$g = \left(1 - a\Omega_2\cos\alpha + a\Omega_1\sin\alpha\right)^2 + a^2\left(\Omega_3 + \frac{\partial\alpha}{\partial s}\right)^2 \ . \tag{S4}$$

A second orthonormal triad can be defined as $\{\hat{\mathbf{p}}_1, \hat{\mathbf{p}}_2, \hat{\boldsymbol{\epsilon}}_3\}$, where $\hat{\mathbf{p}}_2 = \hat{\boldsymbol{\epsilon}}_3 \times \hat{\mathbf{p}}_1$. This frame describes rotation of the PF about the centerline of the CC.

An orthonormal triad for the PF is $\{\hat{\boldsymbol{\epsilon}}_1, \hat{\boldsymbol{\epsilon}}_2, \hat{\boldsymbol{\epsilon}}_3\}$. $\hat{\boldsymbol{\epsilon}}_1$ and $\hat{\boldsymbol{\epsilon}}_2$ are related to $\hat{\mathbf{p}}_1$ and $\hat{\mathbf{p}}_2$ by

$$\hat{\boldsymbol{\epsilon}}_1 = \cos\beta\hat{\mathbf{p}}_1 + \sin\beta\hat{\mathbf{p}}_2 \tag{S5}$$

$$\hat{\boldsymbol{\epsilon}}_2 = -\sin\beta\hat{\mathbf{p}}_1 + \cos\beta\hat{\mathbf{p}}_2 \ . \tag{S6}$$

β is the angle between $\hat{\mathbf{p}}_1$ and $\hat{\boldsymbol{\epsilon}}_1$: It is the PF analog to the CC angle α. A strain vector for the PF, $\boldsymbol{\omega}$ describes the rotation of this triad,

$$\frac{\partial\hat{\boldsymbol{\epsilon}}_i}{\partial s_f} = \boldsymbol{\omega} \times \hat{\boldsymbol{\epsilon}}_i \tag{S7}$$

At this point, it is convenient to work in terms of a rotated CC frame, using the rotated curvatures

$$\Upsilon = \Omega_2\cos\alpha - \Omega_1\sin\alpha \tag{S8}$$

$$\Xi = \Omega_2\sin\alpha + \Omega_2\cos\alpha \ . \tag{S9}$$

Using relations that can be derived from Eq. S7,

$$\omega_1 = -\hat{\boldsymbol{\epsilon}}_2 \cdot \frac{\partial \hat{\boldsymbol{\epsilon}}_3}{\partial s_\mathrm{f}} \quad \text{(S10)}$$

$$\omega_2 = \hat{\boldsymbol{\epsilon}}_1 \cdot \frac{\partial \hat{\boldsymbol{\epsilon}}_3}{\partial s_\mathrm{f}} \quad \text{(S11)}$$

$$\omega_3 = \hat{\boldsymbol{\epsilon}}_2 \cdot \frac{\partial \hat{\boldsymbol{\epsilon}}_1}{\partial s_\mathrm{f}} \ , \quad \text{(S12)}$$

we can derive the curvatures and twist of the PF in terms of $\mathbf{\Omega}$, α, and β,

$$\begin{aligned} \omega_1 &= -\varpi_1 \sin\beta - \varpi_2 \cos\beta \\ \omega_2 &= -\varpi_1 \cos\beta + \varpi_2 \sin\beta \\ \omega_3 &= \frac{1}{\sqrt{g}}\frac{\partial \beta}{\partial s} + \frac{1}{g}\frac{\partial \alpha'}{\partial s} \end{aligned} \quad \text{(S13)}$$

and we have defined

$$\frac{\partial \alpha'}{\partial s} = \frac{\partial \alpha}{\partial s} + \Omega_3 \ , \quad \text{(S14)}$$

$$\varpi_1 = \frac{1}{g}\left(a\left(\frac{\partial \alpha'}{\partial s}\right)^2 - (1 - a\Upsilon)\Upsilon\right) \ , \quad \text{(S15)}$$

$$\varpi_2 = \frac{1}{g^{3/2}}\left(a\frac{\partial^2 \alpha'}{\partial s^2}(1 - a\Upsilon) - g\Xi + a^2\frac{\partial \Upsilon}{\partial s}\frac{\partial \alpha'}{\partial s}\right) \ . \quad \text{(S16)}$$

The forces and torques

When the flagella are not present, the CC has a straight, rod-shaped morphology (3–5). Purified flagella are helical with a helix radius $R = 0.14\ \mu$m and pitch $P = 1.48\ \mu$m (6). Therefore, we treat the CC as a straight filament with no preferred curvature or twist. Using the empirically determined helix radius and pitch, the preferred curvature and torsion of the PF are

$$\kappa_0 = \frac{R}{R^2 + (P/2\pi)^2} = 1.86\ \mu\mathrm{m}^{-1} \quad \text{(S17)}$$

$$\tau_0 = \frac{(P/2\pi)}{R^2 + (P/2\pi)^2} = 3.14\ \mu\mathrm{m}^{-1} \quad \text{(S18)}$$

The internal elastic stresses of the CC exert a force $\mathbf{F}^{\rm c}$ and a moment $\mathbf{M}^{\rm c}$ on the cross section at s. Balancing the forces and moments of an element of the rod of length ds leads to (2)

$$\frac{\partial \mathbf{F}^{\rm c}}{\partial s} + \mathbf{K} = 0 \,, \tag{S19}$$

$$\frac{\partial \mathbf{M}^{\rm c}}{\partial s} + \hat{\mathbf{e}}_3 \times \mathbf{F}^{\rm c} = 0 \,, \tag{S20}$$

where $\mathbf{K} = K\hat{\mathbf{p}}_1$ is the force per length that the PF exert on the CC; i.e., the force that the PF exert on the CC acts along the line connecting the centers of the PF and the CC. Likewise, the elastic stresses of the PF exert a force $\mathbf{F}^{\rm f}$ and a moment $\mathbf{M}^{\rm f}$ on the cross section of the PF that lies at s. Force and moment balance on an element of the PFs of length $\sqrt{g}$ds leads to

$$\frac{1}{\sqrt{g}}\frac{\partial \mathbf{F}^{\rm f}}{\partial s} - \frac{1}{\sqrt{g}}\mathbf{K} = 0 \,, \tag{S21}$$

$$\frac{1}{\sqrt{g}}\frac{\partial \mathbf{M}^{\rm f}}{\partial s} + \hat{\boldsymbol{\epsilon}}_3 \times \mathbf{F}^{\rm f} = 0 \,. \tag{S22}$$

We use linear elasticity theory to define the constitutive relation that defines the elastic restoring moments to the strain vectors. Therefore, the bending moments are linearly related to the curvatures and the twisting moments depend linearly on the twist density. Since the cell cylinder is straight in its undeformed state and the periplasmic flagella are helical,

$$\mathbf{M}^{\rm c} = A_{\rm c}\Omega_1\hat{\mathbf{e}}_1 + A_{\rm c}\Omega_2\hat{\mathbf{e}}_2 + C_{\rm c}\Omega_3\hat{\mathbf{e}}_3 \,, \tag{S23}$$

$$\mathbf{M}^{\rm f} = A_{\rm f}\left(\omega_1 - \kappa_0\right)\hat{\boldsymbol{\epsilon}}_1 + A_{\rm f}\omega_2\hat{\boldsymbol{\epsilon}}_2 + C_{\rm f}\left(\omega_3 - \tau_0\right)\hat{\boldsymbol{\epsilon}}_3 \,, \tag{S24}$$

where $A_{\rm c}$ and $A_{\rm f}$ are the bending moduli for the CC and PF, respectively. $C_{\rm c}$ and $C_{\rm f}$ are the twisting moduli for the CC and PF.

The force and moment balance equations (Eqs. S19 - S22) along with the relationships between the CC material frame and the PF material frame (Eq. S12) comprise a system of 12 equations in 12 unknowns; however, this system of equations can be simplified some using constants of the deformations. First, adding the force balance equations (Eqs. S19 & S21), we find that the total force on the composite structure, $\mathbf{F}^{\rm c}+\mathbf{F}^{\rm f}$, is equal to a constant, which in the absence of external forces, is zero. Therefore, $\mathbf{F}^{\rm f} = -\mathbf{F}^{\rm c} \equiv -\mathbf{F}$.

In a similar fashion, adding the moment balance equations (Eqs. S20 & S22), leads to an equation for the total elastic restoring moment $\mathbf{M}_T$,

$$\mathbf{M}_T \equiv \mathbf{M}^{\mathrm{c}} + \mathbf{M}^{\mathrm{f}} - a\hat{\mathbf{p}}_1 \times \mathbf{F} = \mathbf{c} \ , \tag{S25}$$

where $\mathbf{c}$ is constant. In the absence of external forces and torques, $\mathbf{c} = 0$. Finally, the $\hat{\mathbf{e}}_3$ component of the CC moment balance equation (S20) gives that $\Omega_3 = \Omega_3^0$, where Ω_3^0 is a constant, assuming that the PF are free to slide about the circumference of the CC.

Using the total moment equation (Eq. S25) and the force and moment balance equations for the CC (Eqs. S19 & S20), we get 5 first order differential equations that determine the equilibrium morphology of *B. burgdorferi*,

$$A_{\mathrm{c}}\Xi - A_{\mathrm{f}}\left(\varpi_2 + \kappa_0 \cos\beta\right) = 0 \ , \tag{S26}$$

$$A_{\mathrm{c}}\left(\frac{\partial \Xi}{\partial s} - \Upsilon\frac{\partial \alpha'}{\partial s}\right) - F_2 = 0 \ , \tag{S27}$$

$$A_{\mathrm{c}}\left(\frac{\partial \Upsilon}{\partial s} + \Xi\frac{\partial \alpha'}{\partial s}\right) + F_1 = 0 \ , \tag{S28}$$

$$\frac{\partial F_2}{\partial s} - F_3\Xi + F_1\frac{\partial \alpha'}{\partial s} = 0 \ , \tag{S29}$$

$$\frac{\partial F_3}{\partial s} - F_1\Upsilon + F_2\Xi = 0 \ , \tag{S30}$$

where the force is written in terms of the CC frame, $\mathbf{F} = F_1\hat{\mathbf{p}}_1 + F_2(\hat{\mathbf{e}}_3 \times \hat{\mathbf{p}}_1) + F_3\hat{\mathbf{e}}_3$, and the moment equations (Eq. S25) set the values of F_2 and F_3,

$$F_2 = \frac{A_{\mathrm{f}}}{\sqrt{g}}\frac{\partial \alpha'}{\partial s}\left(\varpi_1 + \kappa_0 \sin\beta\right) + \frac{(1 - a\Upsilon)}{a}\left(\frac{C_{\mathrm{f}}}{\sqrt{g}}\left(\omega_3 - \tau_0\right) - C_{\mathrm{c}}\Omega_3^0\right), \tag{S31}$$

$$F_3 = \frac{A_{\mathrm{f}}}{a\sqrt{g}}\left(1 - a\Upsilon\right)\left(\varpi_1 + \kappa_0 \sin\beta\right) - \frac{A_{\mathrm{c}}}{a}\Upsilon - \frac{\partial \alpha'}{\partial s}\left(\frac{C_{\mathrm{f}}}{\sqrt{g}}\left(\omega_3 - \tau_0\right) - C_{\mathrm{c}}\Omega_3^0\right) \ . \tag{S32}$$

Manipulation of these equations leads to first order equations for Υ and Ξ, and second order equations that determine α' and β:

$$\begin{aligned}
\left(\mathcal{A}g^{3/2}+1\right)\frac{\partial\Upsilon}{\partial s} &= \left(2+\mathcal{A}\sqrt{g}\,(3-g)\right)\Xi\frac{\partial\alpha'}{\partial s}-\Gamma\mathcal{A}g^{3/2}\left(\omega_3-\tau_0\right)\Xi \\
&\quad +\left(\left(\Gamma+1\right)g\omega_3-3\frac{\partial\alpha'}{\partial s}-\Gamma g\tau_0\right)\sqrt{g}\kappa_0\cos\beta \\
&\quad -a\Gamma_{\mathrm{c}}\mathcal{A}\frac{\partial^2\alpha'}{\partial s^2}\Omega_3^0\ , \qquad \text{(S33)}\\
a\left(1-a\Upsilon\right)\frac{\partial^2\alpha'}{\partial s^2} &= \left(\mathcal{A}g^{3/2}+g\right)\Xi-a^2\frac{\partial\Upsilon}{\partial s}\frac{\partial\alpha'}{\partial s}-g^{3/2}\kappa_0\cos\beta\ , \qquad \text{(S34)}\\
\mathcal{A}\frac{\partial\Xi}{\partial s} &= \mathcal{A}\Upsilon\frac{\partial\alpha'}{\partial s}+\frac{1}{\sqrt{g}}\frac{\partial\alpha'}{\partial s}\left(\varpi_1+\kappa_0\sin\beta\right) \\
&\quad +\frac{\left(1-a\Upsilon\right)}{a}\left(\frac{\Gamma}{\sqrt{g}}\left(\omega_3-\tau_0\right)-\Gamma_{\mathrm{c}}\mathcal{A}\Omega_3^0\right)\ , \qquad \text{(S35)}\\
\Gamma\frac{\partial}{\partial s}\left(\omega_3-\tau_0\right) &= \sqrt{g}\kappa_0\left(\varpi_1\cos\beta-\varpi_2\sin\beta\right)\ , \qquad \text{(S36)}
\end{aligned}$$

where $\Gamma = C_{\mathrm{f}}/A_{\mathrm{f}}$, $\Gamma_{\mathrm{c}} = C_{\mathrm{c}}/A_{\mathrm{c}}$, and $\mathcal{A} = A_{\mathrm{c}}/A_{\mathrm{f}}$.

The coefficient before the derivative of Υ in Eq. S33 acts like an effective bending modulus. Therefore, we can estimate the bending modulus of the composite object that consists of the cell and the flagella as

$$A_{\mathrm{eff}} \approx A_{\mathrm{c}} + \frac{1}{g^{3/2}}A_{\mathrm{f}} \qquad \text{(S37)}$$

The equation for Υ (Eq. S33) can be shown to be a total derivative. Integrating this equation leads to,

$$\begin{aligned}
&\mathcal{A}\left(1-a\Upsilon\right)\Upsilon-\sqrt{g}\left(\varpi_1+\kappa_0\sin\beta\right) \\
&+\frac{a\sqrt{g}}{2}\left(\varpi_1^2+\varpi_2^2+\Gamma\omega_3^2-\kappa_0^2-\Gamma\tau_0^2\right)+a\Gamma_{\mathrm{c}}\mathcal{A}\Omega_3^0\frac{\partial\alpha'}{\partial s} = 0\ . \qquad \text{(S38)}
\end{aligned}$$

The first term represents the component of the CC restoring moment along the $\hat{\mathbf{p}}_2$ direction. The second term is the component of the PF restoring moment along the same direction. The third and fourth terms are the moment that arises due to the component of the force along the tangent vector of the PF ($\mathbf{F}\cdot\hat{\boldsymbol{\epsilon}}_3$). In the absence of externally applied moments and forces, the sum of these moments must be zero.

Because the interaction force between the CC and PF acts along the $\hat{\mathbf{p}}_1$ direction, this force can not produce a moment in the $\hat{\mathbf{p}}_1$ direction. This leads to a boundary condition $\Xi = 0$. We also assume that the torque on the flagella about $\hat{\boldsymbol{\epsilon}}_3$ is zero. Finally, because the flagella are subterminally anchored to the cell cylinder and are long enough to overlap in the center of the cell, we treat the flagella as a continuous bundle of filaments that span the length of the cell. As the flagella are anchored to the inner membrane of the cell, we specify the angles that the PFs attach at the ends of the cell. Therefore, the boundary conditions are

$$\begin{aligned} \Xi(s=0) = 0 \ ; &\quad \Xi(s=L) = 0 \\ \omega_3(s=0) = \tau_0 \ ; &\quad \omega_3(s=L) = \tau_0 \\ \alpha(s=0) = 0 \ ; &\quad \operatorname{mod}\left(\frac{\alpha(s=L)}{2\pi}\right) = \alpha_L \ , \end{aligned} \tag{S39}$$

where α_L is the attachment angle of the periplasmic flagella at $s = L$, with respect to the attachment angle at $s = 0$. Our numerical solution of the equations suggest that the morphology of the bacteria is only weakly dependent on this angle. Variation of this angle by $\pm\pi$, leads to variations in the wavelength and amplitude of the morphology on order of 10%.

Small Amplitude Analysis

As the equations that describe the shape of *B. burgdorferi* are fairly complicated and we are expecting a shape that fluctuates about a single axis, we will analyze the equations for small amplitude deformations. We consider the case where the cell cylinder is aligned primarily with the x axis and write its position as

$$\mathbf{r}_{\mathrm{c}} = x\hat{\mathbf{x}} + Y(x)\hat{\mathbf{y}} + Z(x)\hat{\mathbf{z}} \ . \tag{S40}$$

We define that $\hat{\mathbf{e}}_1 = \hat{\mathbf{y}}$ and $\hat{\mathbf{e}}_2 = \hat{\mathbf{z}}$. Therefore,

$$\Omega_1 = -\frac{\partial^2 Z}{\partial x^2} \ , \tag{S41}$$

$$\Omega_2 = \frac{\partial^2 Y}{\partial x^2} \ . \tag{S42}$$

The position of the periplasmic flagella can be written as

$$\begin{aligned} \mathbf{r}_{\mathrm{f}} &= \mathbf{r}_{\mathrm{c}} + a\cos\alpha\hat{\mathbf{y}} + a\sin\alpha\hat{\mathbf{z}} \\ &= x\hat{\mathbf{x}} + (Y(x) + a\cos\alpha)\,\hat{\mathbf{y}} + (Z(x) + a\sin\alpha)\,\hat{\mathbf{z}} \ . \end{aligned} \tag{S43}$$

Defining $\hat{\boldsymbol{\epsilon}}_1 = \cos\beta\hat{\mathbf{y}} + \sin\beta\hat{\mathbf{z}}$ and $\hat{\boldsymbol{\epsilon}}_2 = -\sin\beta\hat{\mathbf{y}} + \cos\beta\hat{\mathbf{z}}$, we find

$$\omega_1 = \varpi_1 \sin\beta - \varpi_2 \cos\beta \ , \tag{S44}$$

$$\omega_2 = \varpi_1 \cos\beta + \varpi_2 \sin\beta \ , \tag{S45}$$

$$\omega_3 = \frac{\partial\beta}{\partial x} \ , \tag{S46}$$

where

$$\varpi_1 = \frac{\partial^2 Y}{\partial x^2} - a\frac{\partial^2\alpha}{\partial x^2}\sin\alpha - a\left(\frac{\partial\alpha}{\partial x}\right)^2\cos\alpha \ , \tag{S47}$$

$$\varpi_2 = \frac{\partial^2 Z}{\partial x^2} + a\frac{\partial^2\alpha}{\partial x^2}\cos\alpha - a\left(\frac{\partial\alpha}{\partial x}\right)^2\sin\alpha \ . \tag{S48}$$

Using these equations, we can write the total energy for the composite structure as

$$\begin{aligned}\mathcal{E} = {} & \frac{A_\mathrm{c}}{2}\int \mathrm{d}x \left(\left(\frac{\partial^2 Y}{\partial x^2}\right)^2 + \left(\frac{\partial^2 Z}{\partial x^2}\right)^2\right) + \frac{C_\mathrm{c}}{2}\int \mathrm{d}x\Omega_3^2 \\ & + \frac{A_\mathrm{f}}{2}\int \mathrm{d}x \left(\varpi_1 - \kappa_0\sin\beta\right)^2 + \left(\varpi_2 + \kappa_0\cos\beta\right)^2 \\ & + \frac{C_\mathrm{f}}{2}\int \mathrm{d}x \left(\frac{\partial\beta}{\partial x} - \tau_0\right)^2\end{aligned} \tag{S49}$$

Minimizing this energy with respect to Y and Z and setting boundary terms to zero, we find

$$\left(1 + \mathcal{A}^{-1}\right)\frac{\partial^2 Y}{\partial x^2} = a\frac{\partial^2\alpha}{\partial x^2}\sin\alpha + a\left(\frac{\partial\alpha}{\partial x}\right)^2\cos\alpha + \kappa_0\sin\beta \ , \tag{S50}$$

$$\left(1 + \mathcal{A}^{-1}\right)\frac{\partial^2 Z}{\partial x^2} = -a\frac{\partial^2\alpha}{\partial x^2}\cos\alpha + a\left(\frac{\partial\alpha}{\partial x}\right)^2\sin\alpha - \kappa_0\cos\beta \ . \tag{S51}$$

A planar solution requires that there exists an angle θ such that $Y\cos\theta + Z\sin\theta = 0$, for all Y and Z. Therefore, from Eqs. S50-S51, we are looking for solutions with

$$a\frac{\partial^2\alpha}{\partial x^2}\sin(\alpha-\theta) + a\left(\frac{\partial\alpha}{\partial x}\right)^2\cos(\alpha-\theta) + \kappa_0\sin(\beta-\theta) = 0 \ . \tag{S52}$$

For a periodic solution, $\partial\alpha/\partial x$ should be roughly constant. Therefore, flat-wave solutions are ones for which $a(\partial\alpha/\partial x)^2 \approx \kappa_0$ and $\alpha \approx -(\beta + \pi/2)$. Minimization of the energy with respect to β gives that $\partial\beta/\partial x = \tau_0 + \mathcal{O}(a\kappa_0)$. Therefore, we expect that flat-wave solutions are ones with $a\tau_0^2 \sim \kappa_0$.

Numerical solution of the mathematical model

We solved Eqs. S33-S36 using the boundary conditions given in Eq. S39 and Eq. S38. We treated Eqs. S34 & S36 as first order equations for α', β, $\partial\alpha'/\partial s$, and $\partial\beta/\partial s$. Eqs. S33 & S35 were solved for Υ and Ξ. These six first order differential equations (Eqs. S33-S36) and an equation for the constant Ω_3^0 were solved simultaneously using the boundary value problem solver in MATLAB (bvp4c), using a relative tolerance of 10^{-6}.

2 Fitting the Experimental Data

Stretching the cell cylinder

The shape of the cell cylinder of *B. burgdorferi* is roughly sinusoidal (4). To fit the data from our cell cylinder stretching experiments, we assume that the CC is sinusoidal. This assumption is also validated by the mathematical model. From the approximate solution given above, Eq. S33 predicts that the preferred curvature of the Υ component of the CC is approximately proportional to $a\tau_0^2 + \kappa_0 \sin 2\tau_0 s$, where we have used $\partial\beta/\partial s \sim 2\tau_0$ and $\partial\alpha/\partial s \sim -\tau_0$. Under the same approximation, the preferred curvature of the Ξ component is zero. The effective bending modulus is, therefore, $A_{\text{eff}} \approx A_{\text{c}} + g^{-3/2}A_{\text{f}} \approx A_{\text{c}} + 0.6A_{\text{f}}$.

The force to stretch an elastic filament that has a sinusoidal preferred shape with N/2 wavelengths a distance $N\Delta L$ is the same force that is required to stretch a filament that is only half a wavelength long a distance ΔL (See Figure 2). Therefore we consider the force-displacement curve for a sinusoidal elastic filament that is one half wavelength long. This curve is generated by solving the Kirchoff rod equations (2),

$$\frac{\partial \mathbf{M}}{\partial s} = \mathbf{F} \times \frac{\partial \mathbf{r}}{\partial s} \tag{S53}$$

$$\frac{\partial \mathbf{F}}{\partial s} = 0 \; , \tag{S54}$$

where $\mathbf{M}$ is the elastic restoring torque, $\mathbf{F}$ is the force on the filament, and $\partial\mathbf{r}/\partial s$ is the tangent vector. In two dimensions, the elastic restoring torque is $A_{\text{eff}}(\kappa - \kappa_0)$, where $\kappa = \partial\theta/\partial s$ is the curvature, with θ the angle between the tangent vector and the x axis. κ_0 is the preferred curvature. For this case, we need to solve

$$A_{\text{eff}} \frac{\partial}{\partial s} \left(\frac{\partial \theta}{\partial s} - \kappa_0 \right) = F \sin\theta \ , \tag{S55}$$

and we use that $\kappa_0 = \tilde{\kappa} \sin ks$, with $\tilde{\kappa}$ a constant. The displacement of the ends of the filament can be found from this equation from

$$\Delta L = \int_0^L \cos\theta \mathrm{d}s - L_0 \ , \tag{S56}$$

where L_0 is the unstressed distance between the ends and L is the total length of the filament. For a half wavelength of filament, $L_0 = \pi/k = \lambda/2$. If the actual CC is N/2 half wavelengths, then the total displacement is $N\Delta L$. Eqs. S35 and S36 can be recast using a non-dimensional length $\tilde{L} = \tilde{\kappa}L$ and force $\tilde{F} = F/A\tilde{\kappa}^2$. In these variables, we generate numerically a force/displacement curve for a filament of length $\lambda/2$. This curve is compared to our data by minimizing

$$\chi^2 = \frac{1}{2} \sum_i \min \left(\left(\Delta L_{exp,i} - c_1 \Delta\tilde{L} - c_2 \right)^2 + \left(F_{exp,i} - c_3 \tilde{F} - c_4 \right)^2 \right) \tag{S57}$$

where the sum is over the experimental data points denoted by ΔL_{exp} and F_{exp}. Here, $c_1 = 2N/\tilde{\kappa}$, $c_3 = A\tilde{\kappa}^2$, and c_2 and c_4 are constants that allow for offsets in the zero positions for F and ΔL. The min function determines the closest point between the ith experimental data point and the numerically generated curve. We estimate $\tilde{\kappa} \approx 1\mu\text{m}^{-1}$ and find the effective bending modulus, A_{eff}, and the number of half wavelengths, N from our fitted values for c_1 and c_3. Minimization of Eq. S57 was done numerically using the MATLAB routine *fminunc*.

Stretching the periplasmic flagella

A similar procedure to that described in the previous section was used to determine the bending modulus of the periplasmic flagella. Since the PFs are known to be helical with preferred curvature and torsion given by Eqs. S15 and S16, we solve Eqs. S53 and S54 using

$$\mathbf{M} = A_{\text{f}} \left(\omega_1 - \kappa_0 \right) \hat{\mathbf{e}}_1 + A_{\text{f}} \omega_2^2 + C_{\text{f}} \left(\omega_3 - \tau_0 \right)^2 \tag{S58}$$

and the relationships given in Eq. S7. From these equations and the known end-to-end distances from the experiments, we calculate the force required to displace the end of the flagellum in the x direction, using clamped boundary conditions (fixed position and tangent vector). The bending modulus and twisting modulus are free parameters that can be used to fit the data. We find that the results are not sensitive to our choice for $2/3 < C_{\mathrm{f}}/A_{\mathrm{f}} < 1$.

References

1. Hovind Hougen, K. (1984) *Yale J. Biol. Med.* **57**, 543-548.

2. Landau, L. D. & Lifshitz, E. M. (1986) Theory of Elasticity, 3rd ed., Pergammon Press, Oxford.

3. Motaleb, M. A., Corum, L., Bono, J. L., Elias, A. F., Rosa, P., Samuels, D.S. , & Charon, N. W. (2000) *Proc. Natl. Acad. Sci. USA* **97**, 10899-10904.

4. Goldstein, S. F., Charon, N. W., & Kreiling, J. A. (1994) *Proc. Natl. Acad. Sci. USA* **91**, 3433-3437.

5. Charon, N.W. & Goldstein, S.F. (2002) *Annu. Rev. Genet.* **36**, 47-73.

6. Charon, N. W., Goldstein, S.F., Block, S. M., Curci, K. & Ruby, J.D. (1992) *J. Bacteriol.* **174**, 832-840.